Virus Research 267 (2019) 1–8

Contents lists available at ScienceDirect

Virus Research

journal homepage: www.elsevier.com/locate/virusres

The ΦCPG1 chlamydiaphage can infect *Chlamydia trachomatis* and significantly reduce its infectivity

Shijuan Wei, Quanzhong Liu, Tingting Lian, Lili Shao*

Dermatology and Venereology Department, Tianjin Medical University General Hospital, No. 154 Anshan Road, Heping District, Tianjin 300052, China

ARTICLE INFO

Keywords:
Recombinant phage pGFP-ΦCPG1
Chlamydiaphage ΦCPG1
Inhibition
CT
GPIC

ABSTRACT

Recent years have seen a significant increase in rates of persistent, antibiotic-resistant infection of *Chlamydia trachomatis (CT)* infections, representing an increasingly serious public health threat. At present there are no effective vaccines or antibodies available to treat *CT*, prompting the need for novel treatment strategies. One potential solution to this issue is the use of ΦCPG1, a *chlamydia*-specific lytic phage which has over 90% nucleotide sequence identity with other chlamydiaphages. Previous work has shown the Vp1 capsid protein of ΦCPG1 to exhibit broad inhibitory activity against all *CT* serotypes, inhibiting *CT*-mediated host cell toxicity. Patients with *CT* infections exhibit circulating antibodies against this Vp1 protein, suggesting that this or similar phages may be present *in vivo* in the context of *CT* infections, even though no phages have been specifically detected to date. Given these previous findings, we hypothesized that the ΦCPG1 chlamydiaphage may be able to infect *CT*, thereby inhibiting its growth and proliferation. To test this, we generated a recombinant pGFP-ΦCPG1 phage which we used to explore its effects on CT and chlamydia conjunctivitis of guinea pigs (*GPIC*). We found that pGFP insertion did not alter the packaging or infectivity of ΦCPG1, and that this recombinant phage was readily able to infect *CT* and *GPIC* and inhibit *CT* and *GPIC* in a dose-dependent fashion. This inhibition was most pronounced during the mid and late stages of the *CT* infection, disrupting the reticular body (RB) to EB transition, leading to the formation of enlarged RBs. These results indicate that ΦCPG1 is able to infect *CT*, highlighting this phage as a novel potential therapeutic agent for treating chlamydia infections. In addition, by engineering pGFP to express ΦCPG1, we have produced an valuable experimental tool useful for future studies of drug resistance, pathogenicity, and vaccine research aimed at improving *CT* treatment.

1. Introduction

As an obligate intracellular bacteria, *Chlamydia trachomatis* (*CT*) has a unique growth cycle that consists of two primary phases - an infectious elementary body (EB) phase during which the bacteria can bind to and infect cells, and a metabolically active reticular body (RB) phase during which the bacteria rapidly proliferates within cells. As the bacteria replicate within cells, they revert to the EB phase and are ultimately released, whereupon they are able to infect new target cells.

Genital *CT* infections remain the leading cause of sexually transmitted infections globally (Filardo et al., 2017), with the CDC reporting 1,708,569 total cases of CT infection in the United States in 2017 alone (Centers for Disease Control and Prevention, 2017). This high rate of CT infections (528.8 per 100,000 persons) represents a striking 6.9% increase over rates in 2016 (Centers for Disease Control and Prevention, 2017). Genital *CT* infections can be extremely deleterious to those infected, causing both immediate symptoms and significantly elevating future susceptibility to both HIV and cervical cancer (Rotchford et al., 2000; Silva et al., 2014). The unique growth and developmental cycle of *CT* renders it less susceptible to traditional antibiotic therapies, and has hindered any efforts to develop an efficacious vaccine against this pathogen (Darville, 2013; Yu et al., 2016). One unique therapeutic strategy aimed at combating *CT* relies upon a Chlamydia-specific bacteriophage, also known as a chlamydiaphage, that is able to infect and disrupt the normal growth characteristics of this pathogenic bacteria. Bacteriophages have long been employed in the field of molecular biology owing to their exquisite specificity, and this same specificity has led to a recent increase in interest in using these phages to target antibiotic-resistant bacteria (Lin et al., 2017).

At present there are six known species of chlamydiaphage: Chp1, Chp2, Chp3, Chp4, chlamydia pneumoniae phage CPAR39 (phiCPAR39), and guinea pig chlamydiaphage (ΦCPG1) derived from

* Corresponding author at: Dermatology and Venereology Department, Tianjin Medical University General Hospital, No. 154 Anshan Road, Heping District, Tianjin 300052, China.
E-mail address: zyypfksjt2014@163.com (L. Shao).

https://doi.org/10.1016/j.virusres.2019.04.008
Received 18 February 2019; Received in revised form 24 April 2019; Accepted 24 April 2019
Available online 25 April 2019
0168-1702/

within the *Chlamydia pneumoniae*, *Chlamydia psittaci*, and *Chlamydia pecorum* species (Storey et al., 1989; Hsia et al., 2000; Liu et al., 2000; Everson et al., 2003; Hoestgaard-Jensen et al., 2011; Sait et al., 2011). At present there has not been any successful detection of a chlamydiaphage associated with *CT*. This may be because *CT* is incompatible with bacteriophages, or because the association of *CT* and its corresponding phages is relatively short in clinical settings, making it difficult to detect owing to the strong inhibitory effects exerted on *CT* by these hypothetical phages.

Research regarding the 6 characterized chlamydiaphages has shown a high degree of homology among them, with the ΦCPG1 phage having greater than 90% sequence homology with the other 5 known phages. Through the study of chlamydiaphage hosts, we have previously determined that there is also a significant overlap with respect to the compatible host species for these chlamydiaphages, such that a given phage is capable of targeting and infecting a range of different *Chlamydia* species (Śliwa-Dominiak et al., 2013).

The Vp1 capsid protein derived from the ΦCPG1 chlamydiaphage has been shown to be able to markedly disrupt the growth and proliferation of *CT* within target cells (Ma et al., 2017), and it can further impair *CT* proliferation *in vivo* in a murine model of genital *CT* infection (Wang et al., 2017). This capsid protein binds in a specific manner to polymorphic membrane protein I (PmpI) of *CT* without interacting with any other known outer membrane proteins (Liu et al., 2012; Ren et al., 2018). We have also previously found that both this Vp1 capsid protein and antibodies against this protein are detectable in the blood of individuals suffering from *CT* infections, suggesting that the ΦCPG1 phage may be capable of infecting *CT* in humans (Ma et al., 2016). Given these previous findings, in the present study we sought to use this ΦCPG1 phage to infect *CT* and explore its specificity for and effects on this pathogen.

2. Materials and methods

2.1. Cell culture

HeLa cells were obtained from the Tianjin Institute of Sexually Transmitted Diseases, China. Cells were cultured in DMEM with 10% fetal bovine serum (FBS, Haoyang, Tianjin, China) at 37 °C in a humidified 5% CO_2 incubator using 24-well plates with or without coverslips, and were later transferred to 6-well plates.

2.2. CT and GPIC infections

For these studies, we employed the standard *CT* serotype E strain, as well as the *Chlamydia* species responsible for Guinea pig inclusion conjunctivitis (*GPIC*). HeLa cells grown in a monolayer in 24-well plates were first treated for 30 min using 30 μg/mL DEAE-D to increase subsequent infectivity. This solution was then exchanged for serum-free media, and *CT* was added to cells, which were then incubated for 30 min. To increase the rate of *CT* adhesion to cells, these plates were next spun for 1 h at 500 ×*g* at 32 °C. After spinning, DMEM containing 10% FBS and 1 mg/L cycloheximide (Sigma) was added to cells, which were then incubated at 37 °C for 44–48 h.

2.3. Recombinant plasmid generation

The pGFPMoPn plasmid was obtained from the Tianjin Institute of Sexually Transmitted Diseases, China, while the pUC57-kan plasmid containing the ΦCPG1 sequence was purchased from GENWIZ (China). The pGFPMoPn and ΦCPG1 constructs were used to amplify DNA sequences encoding pGFP and ΦCPG1, respectively (primer sequences shown in Table 1). We then fused the resultant PCR products with an infusion HD cloning kit (Clontech Laboratories Inc, Mountain View, CA) and transformed the fusion product into competent *Escherichia coli* cells (*DH5α*) as previously described (Liu et al., 2014). We identified colonies expressing GFP via PCR with appropriate primers (Table 1) using the following PCR conditions: initial denaturation at 95 °C for 3 min, followed by 35 cycles of 95 °C for 1 min, 57 °C for 30 s, and 72 °C for 1 min, followed by a final elongation at 72 °C for 8 min. The products of this PCR reaction were then run on a 1.0% agarose gel for visualization, and bacterial colonies positive for the pGFP sequence were selected and partially digested using EcoRI (TianGen, China). These partially digested plasmids were then sequenced in their entirety and transformed into *E. coli* for subsequent amplification. We then used the resultant pGFP-ΦCPG1 plasmid for subsequent transformation experiments.

Table 1
Primer sequences.

Primer	Primer sequences (5'to3')
pGFP-primer1	cctcattgatcatttctaatatcagatctggttctatagtgtcacctaaatc
pGFP-primer2	accggaaaactgagtagaaagtcgacattaatctagatatcgagctcg
ΦCPG1-primer1	tttctactcagttttccggtttgataaaaac
ΦCPG1-primer2	ttagaaatgatcaatgaggcctgg
qPCR-primer1	aagtctttcacagaacatggtgtaa
qPCR-primer2	gttcgtgaccacatcctatcca

2.4. GPIC transformation

Purified *GPIC* EBs (1×10^7IFU) were combined at room temperature with 7 μg of the pGFP-ΦCPG1 plasmid in 200 μl CaCl2 buffer for 45 min. A total of 6×10^6 freshly resuspended HeLa cells in 200 μl CaCl2 buffer were then added to this EB/plasmid mixture for an additional 20 min, after which this mixture was plated in 6-well plates containing warmed DMEM + 10% FBS without any additional supplements. After a 12 h incubation to facilitate cell adherence, media was replaced with fresh DMEM containing 10% FBS as well as cycloheximide (2 mg/ml) and ampicillin (5 mg/ml) (Sigma, St. Louis, MO). After a further 36 h incubation, sucrose phosphate amino acid buffer (SPG) was used to collect transformed cells, which were transferred onto fresh HeLa monolayers in the presence of ampicillin (10 μg/ml). This passaging of the *GPIC* cells was repeated 5 times, for a total of 6 generations. At each generation collection time point, DNA was extracted from *GPIC* cultures for use in qualitative and quantitative PCR reactions to confirm the degree of transformation success. Phage DNA in these samples were amplified with qPCR-primer1 and qPCR-primer2 (primer sequences shown in Table 1), which do not amplify any residual phage DNA remaining in chlamydia genomes. PCR conditions were as follows: initial denaturation at 95 °C for 3 min followed by 35 cycles of 95 °C for 1 min, 55 °C for 30 s, and 72 °C for 1 min, followed by a final elongation at 72 °C for 8 min. For quantitative PCR, pGFP-ΦCPG1 plasmid DNA was used for standardization. For qualitative PCR, samples were visualized using a 1.0% agarose gel, with the expected amplified ΦCPG1 fragment being 120 bp in size.

2.5. pGFP-ΦCPG1 phage purification and quantification

At 48 h post-infection, pGFP-ΦCPG1-infected *GPIC* cultures were centrifuged at 30,000 x*g* for 30 min at 4 °C and were filtered using a 0.22 μm membrane to collect the phages present in the supernatant fraction. Purified phage DNA was extracted with a DNA viral genome extraction kit. This DNA was then used to perform quantitative PCR reactions in order to quantify phage levels, using the qPCR-primer1 and qPCR-primer2 listed in Table 1.

2.6. CCK-8 assay

To assess cell viability in our experimental system, we conducted a CCK-8 assay as follows: 10 μL of the provided reagent was combined with 0.1 mL of growth medium and added to HeLa cells incubated with and without phage in 96-well plates. After a 1–4 h incubation period, a

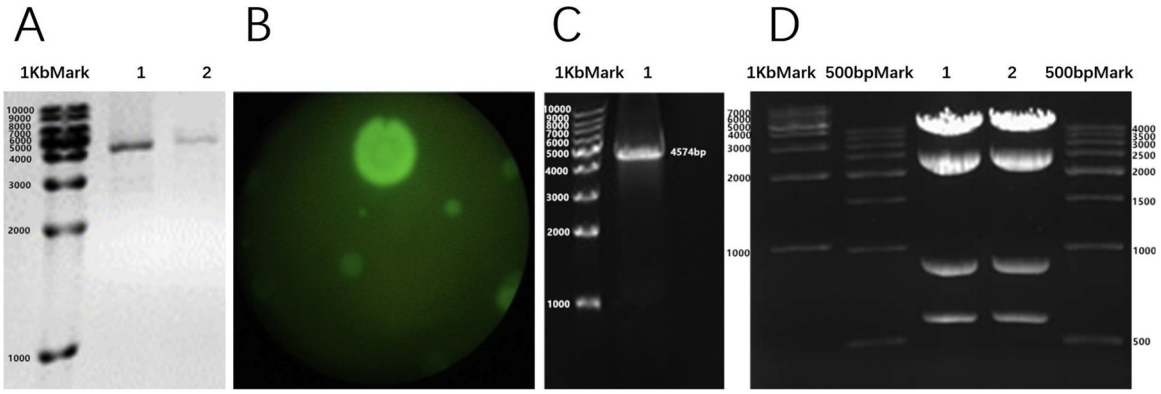

Fig. 1. Construction and identification of the pGFP-ΦCPG1 recombinant plasmid. A. PCR-based analysis of amplified pGFP and ΦCPG1, which were amplified from pGFPMoPn and ΦCPG1 in pUC57-kna, as shown in lane 1 and lane 2, respectively. B. Recombinant phage clones were used to transform *E. coli*, and green fluorescent bacteria were detected via fluorescence microscopy to confirm the presence of positive clones. C. PCR-based verification of the successful ΦCPG1 amplification from the chosen positive clone, following electrophoresis on a 1.0% agarose gel, yielding a positive 4574bp band. D. Lane 1-2, positive result of the recombinant phage M13-IN5 clones digested by the enzyme EcoR1 and analyzed by electrophoresis for 4 expected bands of the following sizes: 4830 bp, 2515 bp, 897 bp, and 603 bp.

microplate reader was used to quantify absorbance at 450 nm. All samples were assayed in triplicate.

2.7. In vitro studies

2.7.1. Dose-dependent phage effects on chlamydia

Hela cells were combined with the recombinant as well as *CT* or *GPIC* cells (10^6 IFU/mL). For phage infection, stock phages was diluted in a total volume of 200 μL cell media to a final concentration of 10^{13}v.g/L, 10^{14}v.g/L, 10^{15}v.g/L, 10^{16} v.g/L, 10^{17}v.g/L, or 10^{18} v.g/L. These phage samples were then combined with CT or GPIC lysates for 1 h at room temperature to yield a *CT/GPIC* mixture. This mixture was then used to infect 80% confluent HeLa monolayers in 24-well plates, with coverslips, as above, for 2 h at room temperature. After 44–48 h, cells were fixed and fluorescence microscopy was used to visualize and count inclusion bodies in cells.

2.7.2. Studies of the effects of phage hyperinfection

We combined uninfected *CT* or *GPIC* with the phage-enriched lysates for 1 h at room temperature, combining 10^6 IFU/mL of CR/GPIC with 10^{16}v.g/L phage. This infectious mixture was then added to prepared HeLa cell monolayers, and samples were collected at 0, 12, 24, 36, 48, 60, 72, 96and 120 h post infection (p.i.) for quantitative PCR and immunofluorescent analyses.

2.7.3. Fluorescence microscopy

We conducted fluorescent imaging as described in previous studies (Ma et al., 2016). Briefly, we collected the coverslips from appropriate wells and fixed cells for 10 min using methanol chilled to −20 °C. Samples were then washed 3 times. To detect inclusion bodies, rabbit anti-*CT* or anti-*GPIC* EB antibodies (1:1000) were used to probe cells overnight at 4 °C, followed by a Dylight-488-conjugated secondary goat anti-rabbit IgG (1:500; Abbkine) at room temperature for 1 h. DAPI was then used for nuclear staining, and cells were visualized by fluorescence microscopy. All assays were conducted in triplicate.

2.8. Transmission electron microscopy (TEM)

HeLa cells infected with *CT* or *GPIC* with or without recombinant phage for 36 h were washed once with PBS and then fixed for 2–3 days at 4 °C using 1.6% glutaraldehyde in phosphate buffer, pH 7.4. Cells were then washed thrice and post-fixed using 1% osmium tetroxide and 1% potassium ferrocyanide. Cells were then washed two times and allowed to rest overnight in distilled water. Samples then underwent graded ethanol dehydration, and were embedded in an epoxy resin. Horizontal sections (70 nm) along the plane of growth were then cut using a diamond knife. These sections were collected in regular 200-mesh copper grids, and uranyl acetate and lead citrate were used for contrast. A Hitachi HT 7700 electron microscope was then used to visualize samples, operating at 80 kV under standard conditions.

2.9. Data analysis

GraphPad Prism version 5.0 for Windows (GraphPad Software, La Jolla California USA, www.graphpad.com) was used to create artwork and to analyze all data. Data analysis was performed using the student's *t*-test. Unless stated otherwise, results are presented as means ± SEM or as percentages. Significance was defined as a value of $p < 0.05$.

3. Results

3.1. Genetic engineering of the pGFP-ΦCPG1 phage

In order to generate a chlamydiaphage expressing GFP, we amplified and fused DNA segments encoding pGFP and ΦCPG1 derived from appropriate constructs, allowing us to generate the appropriate plasmids (Fig. 1A). We then confirmed the successful generation of this plasmid via screening transformed bacterial clones to identify those positive for pGFP expression (Fig. 1B), confirming the successful generation of the pGFP-ΦCPG1 construct. This was further confirmed based on PCR screening of bacterial clones, identifying a 4500bp band consistent with the expected size of the full construct (Fig. 1C). Further confirming that the construct had been successfully generated, it was cleaved into four segments using EcoRI, as expected, yielding 4830bp, 2515bp, 897bp, and 603bp fragments (Fig. 1D).

3.2. GPIC transformation

We next used the $CaCl_2$ method to transform *GPIC* EBs with the recombinant plasmid and confirmed by PCR that these bacteria had been successfully transformed, as evidenced by a 4500bp band only in *GPIC* samples which had been combined with phage DNA (Fig. 2A). Quantitative PCR further confirmed that as these *GPIC* cells were continuously passaged, the number of phage genomes increased (Fig. 2B). These results confirmed the successful packaging of a GFP-expressing ΦCPG1 phage which can be propagated in *GPIC*. This recombinant phage was titered via qPCR, revealing a titer of 6.47×10^{20} v.g/L.

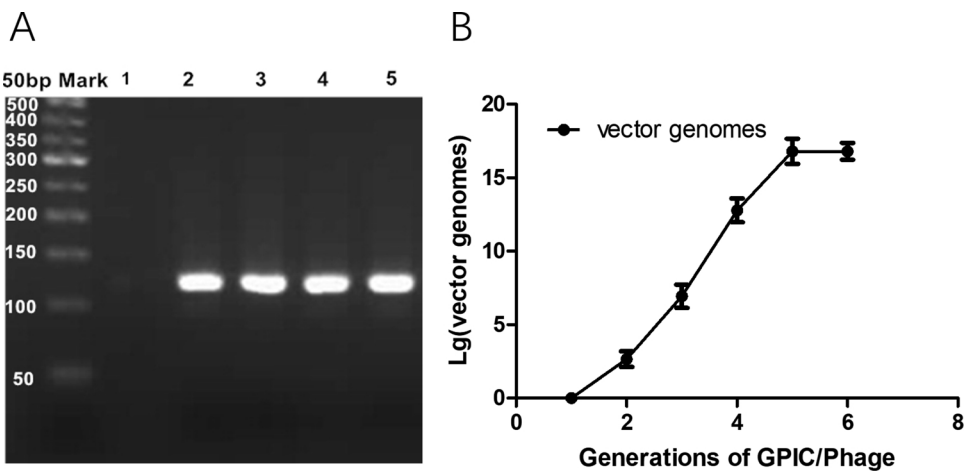

Fig. 2. Confirmation of pGFP-ΦCPG1 phage growth in GPIC cells. A. PCR screening was used to assess the incorporation of the recombinant pGFP-ΦCPG1 into GPIC cells. Lanes 2–5 represent generation 4, generation 5, generation 6, and purified recombinant phage, respectively. Lane 1 represents GPIC cells that were not transformed. B. Recombinant phage titers were measured by qPCR at each generation of GPIC cell passage for 6 total generations.

3.3. pGFP-ΦCPG1 inhibits CT and GPIC proliferation

When we infected *CT* and *GPIC* cells with the recombinant pGFP-ΦCPG1 phage, we determined that infection with this phage was sufficient to inhibit the proliferation of these strains of chlamydia (Fig. 3A–C). This inhibition was dose-dependent, with phage titers below 10^{14}v.g/L producing no detectable inhibitory effect. Titers greater than 10^{14}v.g/L lead to increased inhibition of *CT/GPIC* cell proliferation, with a maximal inhibition at 10^{17}v.g/L (Fig. 3A-C). The effect on GPIC was stronger than that on CT (Fig.3C).We subsequently used this phage at a titer of 10^{16} v.g/L in the following experiments. A CCK-8 assay further confirmed that these phages did not induce HeLa cell toxicity when combined with HeLa cells and *CT* (10^{16} v.g/L) (Fig. 3D). However, as the titer of the recombinant phage increased, the cell viability decreased, which may be due to the increased osmotic pressure caused by the high-titer phage, resulting in cell damage.

3.4. Developmental stage-dependent effects of pGFP-ΦCPG1 on chlamydia infection

To better explore how the pGFP-ΦCPG1 phage affects Chlamydia and the underlying molecular mechanisms governing these effects, we next assessed how this phage influenced different stages of the *CT* developmental cycle. We found that relative to HeLa cells infected with *CT* alone, *CT* development at early time points (up to 12 h post-infection) was not significantly affected by phage infection (Fig. 4A,C,D). In the mid and late stages of *CT* development, however, *CT* proliferation was impaired as evidenced by a significant decrease in the number of inclusion bodies detectable at these time points (24–48 h p.i. Fig. 4A,C,D). There was also a significant delay in the time of peak *CT* inclusion body formation in these phage infected cells (Fig. 4A, C,D). However, beyond about 72 h post-infection the results of the infection were comparable for phage-free vs phage conditions (Fig. 4A). Comparable effects were observed when HeLa cells were co-infected with *GPIC* and this recombinant phage (Fig. 4B,E,F).

3.5. TEM validation of phage infectivity

In order to observe ultrastructural changes in HeLa cells co-infected with chlamydia and pGFP-ΦCPG1, we next performed transmission electron microscopy of cells at the mid-cycle 36 h stage of infection. We observed several detectable differences between the phage-infected and uninfected control cells. We were able to detect smaller pGFP-ΦCPG1-containing chlamydia inclusions in infected cells (Fig. 5B and E) than in uninfected controls (Fig. 5A and D). We were not able to detect the large inclusions typically seen in phage-free cultures at this 36 h time point in phage-containing cultures, indicating the presence of fewer chlamydiae in these cells. While informative, this approach to assessing a phage-dependent loss of inclusions is not quantitative, and is potentially prone to artifacts, necessitating caution when interpreting these results.

We were also able to detect the formation of abnormal forms present only within pGFP-ΦCPG1-infected cultures. Indeed, we observed enlarged RBs termed maxi-RBs (mRBs), that were 2–5x larger than normal RBs (Fig. 5B,C; E,F) in phage-infected cultures, while these were absent in phage-free *GPIC* cultures (Fig. 5).

4. Discussion

There is an ongoing research effort aimed at understanding the biology of genital *CT* infections. As these infections can be difficult to treat and cause serious complications, there is an urgent need for the development of novel disease control measures suited to combatting *CT* infections in the general population. Chlamydiaphages, with their high degree of specificity and ability to disrupt *CT* infectivity in model system, represent an attractive opportunity to develop a novel treatment modality for this serious sexually transmitted infection.

While specific bacteriophages have been isolated from certain Chlamydia strains including *Chlamydia pneumoniae, Chlamydia psittaci,* and *Chlamydia pecurum*, there have not been any reports to date of the isolation of a specific phage associated with the pathogenic *CT* strain. While this does not preclude the existence of such a phage, it may be that if one exists it is likely deleterious to *CT* growth and infection, complicating efforts to detect it in the context of a dynamic infection. With respect to Chlamydia phylogeny, *C. psittaci* and *CT* are evolutionarily older and more closely related than the more recent and simpler *C. pneumoniae* species. This suggests that any phages associated with *CT* may more closely resemble those infecting *C. psittaci.*

The chlamydiaphage ΦCPG1, which is the first such phage able to infect cells in mammals, is known to have greater than 90% sequence homology to other chlamydiaphages. The Vp1 capsid protein from this phage has been shown to inhibit multiple *CT* serotypes, and both Vp1 and antibodies against this protein have been detected in the blood of *CT* patients. Given that there is an overlap in the host range of chlamydiaphages, we therefore hypothesized that the ΦCPG1 phage would be able to infect *CT* and disrupt its proliferation and infectivity.

To test this hypothesis and explore the related biology, we generated a recombinant form of the ΦCPG1 phage encoding pGFP, allowing for easier selection for the phage, screening for clones, and monitoring infected cells in a dynamic environment. We did not detect any changes in phage packaging, proliferation, or infection in *GPIC* cells as a consequence of pGFP insertion. Indeed, the recombinant pGFP-ΦCPG1 phage was able to infect and impair the growth and proliferation of *GPIC* cells, disrupting the RB-to-EB transition during the infectious life

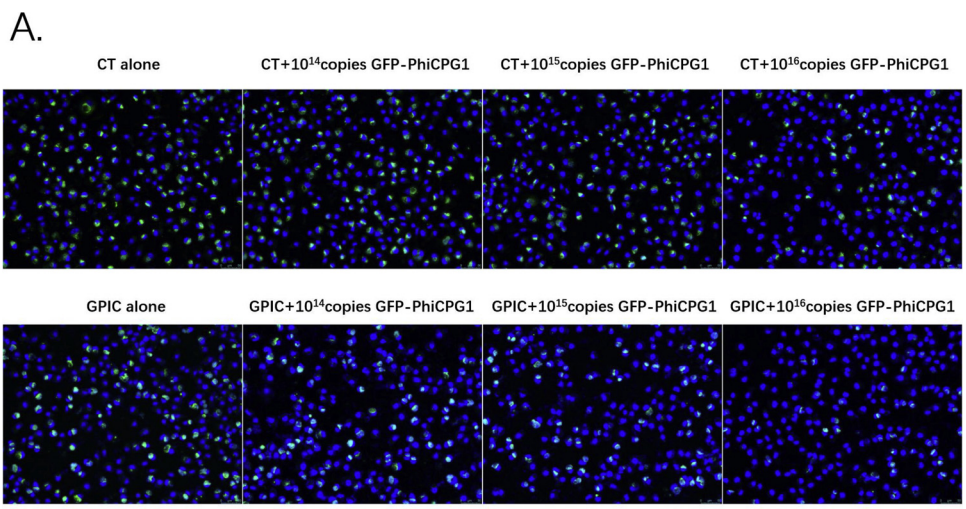

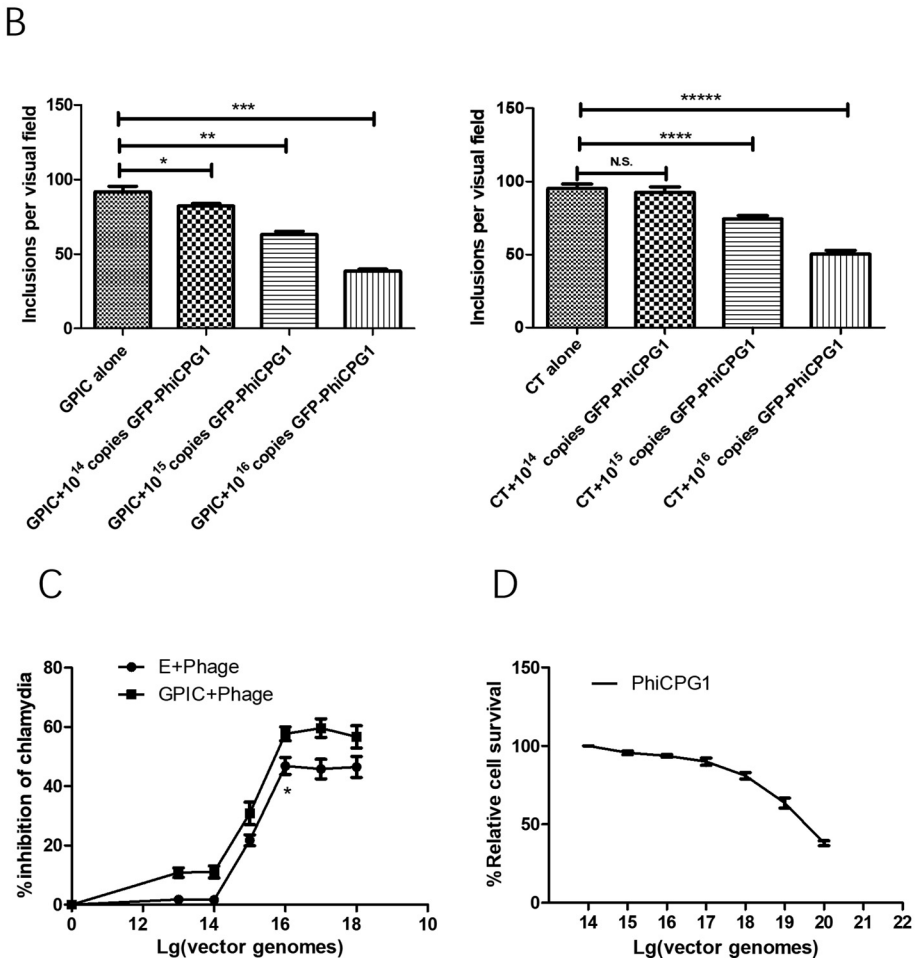

Fig. 3. Dose-dependent effects of pGFP-ΦCPG1 on CT proliferation. GPIC and CT. *Chlamydia* cells were combined with the indicated titers of the pGFP-ΦCPG1 phage, and these cells were then used to infect HeLa cells. The number of inclusions in these HeLa cells was then visualized by fluorescence microscopy after 48 h. The inhibitory effects on GPIC were found to be stronger than that on CT. Fig. 3A and B: *P1 = 0.0487; **P2 = 0.0002; ***P3 < 0.0001; N.S. P1 = 0.6063 ; ****P2 = 0.0007; *****P3 < 0.0001; Blue: DAPI; Green: chlamydia inclusions. Fig. 3C: The effect of the GFP-PhiCPG1 at 10^{16} v.g/L on GPIC was stronger than that on CT, *P < 0.0001. Fig. 3D demonstrates the dose-dependent influence of these phages on the activity of Hela cells.

cycle of this bacteria, and all of these properties of recombinant phages are the same as those of the Chlamydiaphage ΦCPG1(Hsia et al., 2000; Śliwa-Dominiak et al., 2013). This finding suggested that the recombinant phage were comparable to those of the unmodified ΦCPG1 phage, making it a suitable experimental tool for these studies.

When we infected *CT* cells with our recombinant phage, we found to the phage to strongly inhibit *CT* growth much as it did that of *GPIC*, with stronger inhibition as the phage dose increased (Fig. 3). The effect on *GPIC* was stronger than that on *CT*, which may be due to slight differences in the surface receptors bound by ΦCPG1 between these two strains, given that surface protein-protein interactions are the primary mechanisms by which chlamydiaphages infect their target cells. *GPIC* cells may also exhibit a higher density of these target proteins on their surface, increasing their frequency of infection by these phages, while *CT* may have evolved to be more resistant to these phages over time, reducing the consequent lethality of infection with these phages.

When we investigated the dynamics of recombinant phage infections and their effects on *CT* infectivity, we found that this phage did not alter the early stages of *GPIC/CT* infection of HeLa cells, but the mid and late stages of infection were disrupted by the phage(Fig.4). These

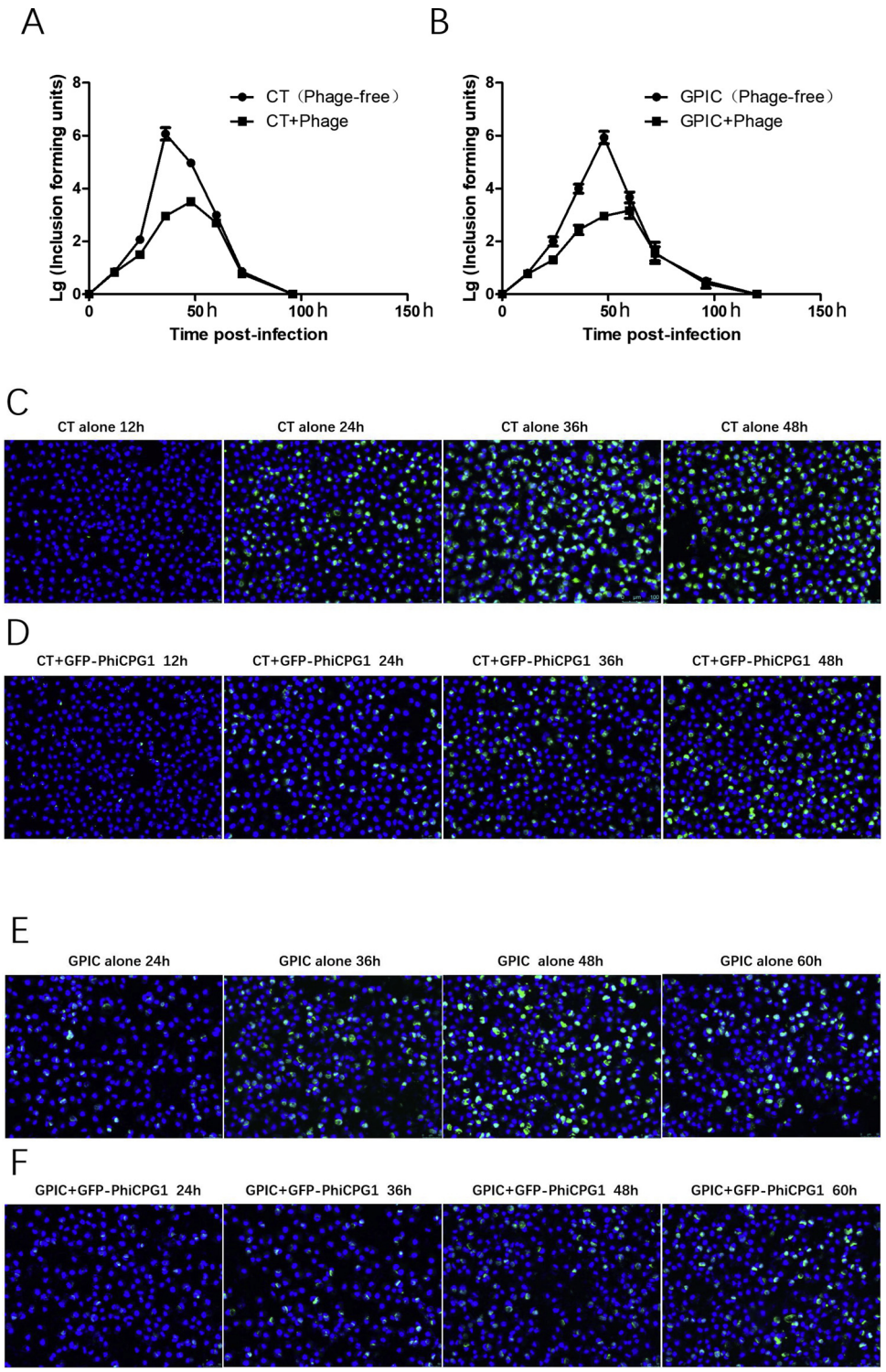

Fig. 4. Developmental stage-dependent effects of pGFP-ΦCPG1 on chlamydia infection.
A,C,D: HeLa cells were infected with CT in the presence or absence of recombinant phage, and inclusion body formation was visualized over time by fluorescence microcopy. B,E,F: HeLa cells were infected with GPIC in the presence or absence of recombinant phage, and inclusion body formation was visualized over time by fluorescence microcopy. For all infections, HeLa cells were mixed with 10^6 IFU *Chlamydia* and 10^{16}v.g/L recombinant phage DNA. Blue: DAPI; Green: *Chlamydia* inclusions.

phases of the infectious cycle are those during which RBs undergo a transformation into EBs, indicating clear disruptions to normal *GPIC/CT* infectivity which also corresponded to a delay in the peak time of observed inclusion body numbers in infected HeLa cells. However, beyond about 72 h post-infection, the results of the infection were comparable for the phage-free and phage-infected samples (Fig. 4). This may be because the conversion between mRB and RB is reversible (Hsia et al., 2000). With the extension of infection time, phage efficacy against *Chlamydia trachomatis* may be weakened or lost due to the death of phage in the external environment, after which mRBs undergo conversion into RBs. When we analyzed ultrastructural changes associated with recombinant phage infection via TEM, we found that during the

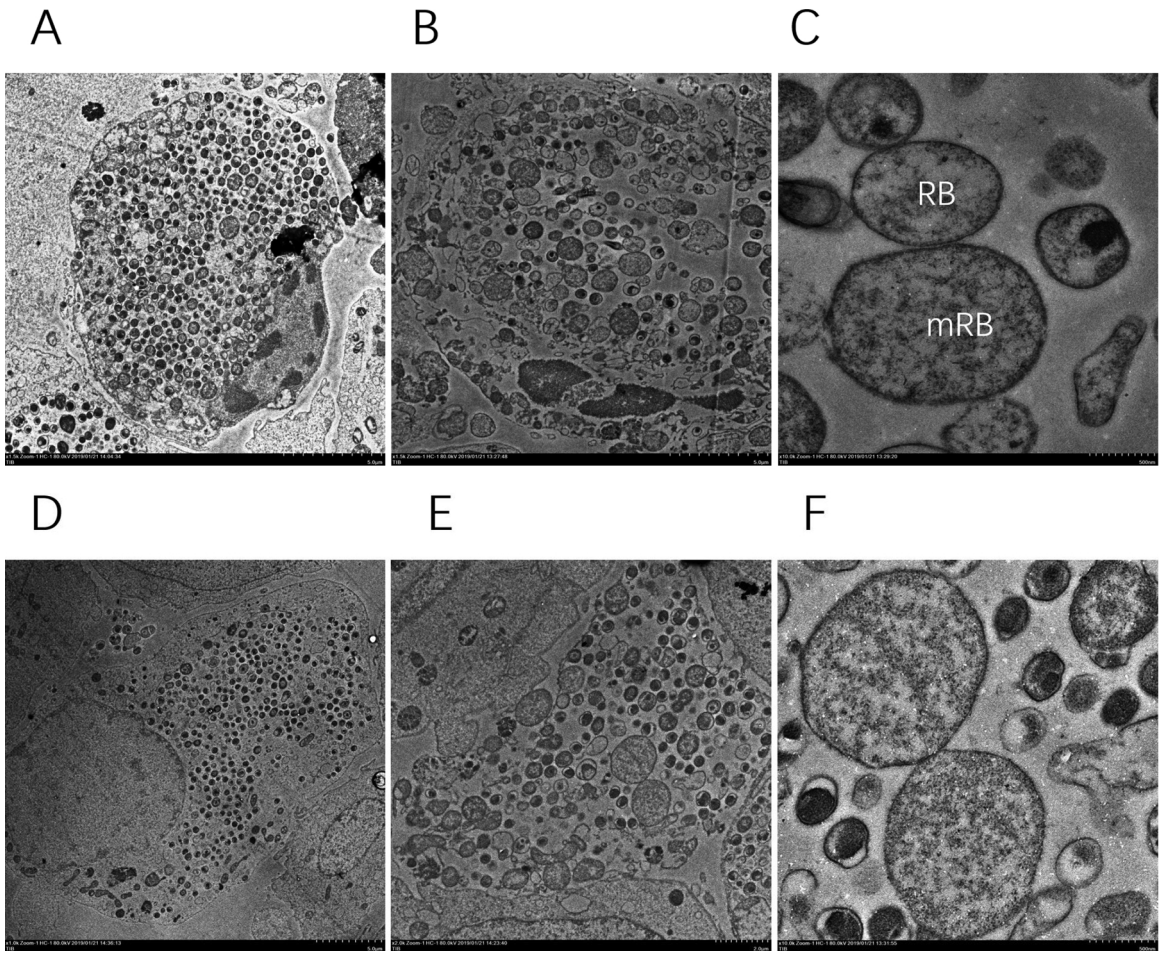

Fig. 5. TEM of phage-infected CT/GPIC inclusion bodies in HeLa cells. TEM staining was used to assess the ultrastructural effects of ΦCPG1-hyperinfection on CT/GPIC 36 h post-infection. CT inclusions in pGFP-ΦCPG1-hyperinfected HeLa cells (B,E) were smaller and contained fewer *Chlamydia* than in cells not infected with phage (A,D). Abnormally enlarged maxi-RBs (mRBs) were evident in these phage-infected cells (B,E), as was evident under higher magnification (C,F).

mid and late stages of infection there was a decrease in both the number and size of inclusion bodies in phage-infected Chlamydia cells, and there were also abnormally enlarged RBs (mRBs) within these inclusion bodies that were absent in phage-free samples(Fig. 5). These enlarged RBs were similar to those structures previously reported in response to IFNγ, amino acid deprivation, or penicillin treatment (Hsia et al., 2000). The similarity of these changes in inclusion body numbers and morphology, as well as a corresponding decrease in infectious yields, suggests that abnormal RB development may be a common feature of Chlamydia responses to a variety of stress-inducing stimuli. As the Vp1 capsid protein is the primary virulence factor associated with chlamydiaphages and is important for host cell recognition, the growth of both phage and host cells should mirror each other to an extent. We hypothesize that our recombinant phage acts on *CT* cells in a manner similar to that previously reported for the Vp1 protein alone, which weakens the activity of the type III secretory system in *CT* cells. During the later stages of the *CT* infectious cycle, increases in the homozygous fusion of RBs can lead to an abnormally enlarged reticulum, adversely impacting RB-to-EB transformation and consequently inhibiting *CT* proliferation (Guo et al., 2016). Our studies of this ΦCPG1 phage suggest that it is likely attenuating the progression of *CT* infections via reducing infectious EB yields. Our ultrastructural approach, however, was not quantitative, and as inclusion size can vary over time future studies will be needed to definitively confirm this hypothesis and to validate our findings.

It is important to note that these in vitro phage growth data cannot be used to draw conclusions regarding their in vivo use. In consideration of a large number of factors, including the substantial loss of phages under non-natural growth conditions, changes in osmotic pressure in the presence of high phage doses thereby affecting, and experimental efficacy, the optimal recombinant phage concentration was determined to be 10^{16}v.g/Lin this study. As *Chlamydia* infections in vivo differ in many ways from those in vitro, this concentration cannot be directly translated into in vivo use. Instead, the optimal therapeutic concentration of the recombinant phage for use in vivo will need to be determined in light of the ability of the immune system to eliminate foreign pathogens.

5. Conclusion

We found that the growth and infectious characteristics of the recombinant pGFP-ΦCPG1 phage were comparable to those of the Chlamydia bacteriophage ΦCPG1, indicating that this recombinant phage is suitable for use in experimental studies in place of ΦCPG1. The pGFP-ΦCPG1 phage was able to readily infect *CT* cells and significantly inhibit their growth and proliferation, indicating that *CT* is a suitable host for this bacteriophage, and that *CT* may be associated with its own closely related bacteriophages. As such our study provides a theoretical foundation for the identification and characterization of phages specific for *CT*.

The identification of novel bacteriophages represents an invaluable approach to both understanding the molecular biology of *CT* and to identifying potential phage-based therapeutic strategies aimed at controlling this disease. The ability of specific phages to mediate *CT* killing

offers a potential means of treating patients suffering from antibiotic-resistant *CT*. In addition, given their high specificity, bacteriophages can be used to study pathogens that are poorly characterized or difficult to isolate, such as *Chlamydia trachomatis*, and as such they represent an optimal tool for exploring the mechanisms governing pathogenicity, providing an opportunity to better investigate the incompletely understood biology of *Chlamydia* and related pathogenic bacteria.

Author contributions

Conceptualization and Methodology: Shijuan Wei and Lili Shao. Formal analysis and Validation: Shijuan Wei and Quanzhong Liu. Formal analysis: Tingting Lian. Resources: Quanzhong Liu and Lili Shao. Writing-Original draft: Shijuan Wei.

Conflicts of interest

The authors declare no conflicts of interest.

Acknowledgments

This research was supported by a grant from the National Natural Science Foundation of China (Grant No.: 31500157).

References

Centers for Disease Control and Prevention, 2017. 2017 Sexually Transmitted Diseases Surveillance. (Accessed 24 July 2018). https://www.cdc.gov/std/.

Darville, T., 2013. Recognition and treatment of chlamydial infections from birth to adolescence. In: Curtis, N., Finn, A., Pollard, A. (Eds.), Hot Topics in Infection and Immunity in Children IX. Springer, New York, NY, pp. 109–122.

Everson, J.S., Garner, S.A., Lambden, P.R., Fane, B.A., Clarke, I.N., 2003. Host range of chlamydiaphages φCPAR39 and Chp3. J. Bacteriol. 185, 6490–6492. https://doi.org/10.1128/JB.185.21.6490-6492.2003.

Filardo, S., Di Pietro, M., Porpora, M.G., Recine, N., Farcomeni, A., Latino, M.A., Sessa, R., 2017. Diversity of cervical microbiota in asymptomatic Chlamydia trachomatis genital infection: a pilot study. Front. Cell. Infect. Microbiol. 7, 321. https://doi.org/10.3389/fcimb.2017.00321.

Guo, Y., Guo, R., Zhou, Q., Sun, C., Zhang, X., Liu, Y., Liu, Q., 2016. Chlamydiaphage φCPG1 capsid protein Vp1 inhibits *Chlamydia trachomatis* growth via the mitogen-activated protein kinase pathway. Viruses 8, 99. https://doi.org/10.3390/v8040099.

Hoestgaard-Jensen, K., Christiansen, G., Honoré, B., Birkelund, S., 2011. Influence of the Chlamydia pneumoniae AR39 bacteriophage φCPAR39 on chlamydial inclusion morphology. FEMS Immunol. Med. Microbiol. 62, 148–156. https://doi.org/10.1111/j.1574-695X.2011.00795.x.

Hsia, R.C., Ohayon, H., Gounon, P., Dautry-Varsat, A., Bavoil, P.M., 2000. Phage infection of the obligate intracellular bacterium, *Chlamydia psittaci* strain guinea pig inclusion conjunctivitis. Microb. Infect. 2, 761–772. https://doi.org/10.1016/S1286-4579(00)90356-3.

Lin, D.M., Koskella, B., Lin, H.C., 2017. Phage therapy: an alternative to antibiotics in the age of multi-drug resistance. World J. Gastrointest. Pharmacol. Ther. 8, 162–173. https://doi.org/10.4292/wjgpt.v8.i3.162.

Liu, B.L., Everson, J.S., Fane, B., Giannikopoulou, P., Vretou, E., Lambden, P.R., Clarke, I.N., 2000. Molecular characterization of a bacteriophage (Chp2) from *Chlamydia psittaci*. J. Virol. 74, 3464–3469. https://doi.org/10.1128/JVI.74.8.3464-3469.2000.

Liu, Y., Sun, Y., Yao, W., Li, Y., Li, Z., Wei, J., Liu, Q., 2012. The detection of the binding protein of chlamydiaphage phiCPGl capsid protein Vpl on chlamydial outer membrane of serotype D. Chin. J. Infect. Dis. 32, 583–586 (In Chinese).

Liu, Y., Chen, C., Gong, S., Hou, S., Qi, M., Liu, Q., Baseman, J., Zhong, G., 2014. Transformation of *Chlamydia muridarum* reveals a role for Pgp5 in suppression of plasmid-dependent gene expression. J. Bacteriol. 196, 989–998. https://doi.org/10.1128/JB.01161-13.

Ma, J., Liu, Y., Liu, Y., Li, L., Hou, S., Gao, X., Qi, M., Liu, Q., 2016. The presence of Chlamydia phage PhiCPG1 capsid protein VP1 genes and antibodies in patients infected with Chlamydia trachomatis. Acta Biochim. Pol. 63, 501–504.

Ma, J., Sun, Y., Sun, C., Zhou, Q., Qi, M., Kong, J., Wang, J., Liu, Y., Liu, Q., 2017. Identification of proteins differentially expressed by *Chlamydia trachomatis* treated with chlamydiaphage capsid protein VP1 during intracellular growth. Arch. Microbiol. 199, 1121–1131. https://doi.org/10.1007/s00203-017-1381-2.

Ren, J., Lian, T., Shao, L., Liu, Y., Liu, Q., 2018. PmpI antibody reduces the inhibitory effect of Vp1 on *Chlamydia trachomatis* infectivity. Can. J. Microbiol. 64, 376–384. https://doi.org/10.1139/cjm-2018-0056.

Rotchford, K., Strum, W.A., Wilkinson, D., 2000. Effect of coinfection with STDs and of STD treatment on HIV shedding in genital-tract secretions: systematic review and data synthesis. Sex. Transm. Infect. 27, 243–248.

Sait, M., Livingstone, M., Graham, R., Inglis, N.F., Wheelhouse, N., Longbottom, D., 2011. Identification, sequencing and molecular analysis of Chp4, a novel chlamydiaphage of *Chlamydophila abortus* belonging to the family *Microviridae*. J. Gen. Virol. 92, 1733–1737. https://doi.org/10.1099/vir.0.031583-0.

Silva, J., Cerqueira, F., Medeiros, R., 2014. *Chlamydia trachomatis* infection: implications for HPV status and cervical cancer. Arch. Gynecol. Obstet. 289, 715–723. https://doi.org/10.1007/s00404-013-3122-3.

Śliwa-Dominiak, J., Suszyńska, E., Pawlikowska, M., Deptuła, W., 2013. Chlamydia bacteriophages. Arch. Microbiol. 195, 765–771. https://doi.org/10.1007/s00203-013-0912-8.

Storey, C.C., Lusher, M., Richmond, S.J., 1989. Analysis of the complete nucleotide sequence of Chp1, a phage which infects avian Chlamydia psittaci. J. Gen. Virol. 70, 3381–3390. https://doi.org/10.1099/0022-1317-70-12-3381.

Wang, S., Guo, R., Guo, Y.L., Shao, L.L., Liu, Y., Wei, S.J., Liu, Y.J., Liu, Q.Z., 2017. Biological effects of chlamydiaphage phiCPG1 capsid protein Vp1 on *chlamydia trachomatis in vitro* and *in vivo*. J. Huazhong Univ. Sci. Technol. Med. Sci. 37, 115–121. https://doi.org/10.1007/s11596-017-1704-1.

Yu, H., Karunakaran, K.P., Jiang, X., Brunham, R.C., 2016. Subunit vaccines for the prevention of mucosal infection with Chlamydia trachomatis. Expert Rev. Vaccines 15, 977–988. https://doi.org/10.1586/14760584.2016.1161510.